Mon. Not. R. astr. Soc. (1987) **227**, 943–965

An infrared study of the stellar population in the direction of the Carina nebula: NGC 3372

Robert G. Smith* *School of Physics (RAAF Academy), University of Melbourne, Parkville, Victoria 3052, Australia*

Accepted 1987 March 23. Received 1987 March 23; in original form 1986 September 5

Summary. Surveys at 2μm have been used to identify the brightest members of the stellar population in the direction of the Carina nebula. Subsequent *JHK* photometry combined with low-resolution 2μm spectra has been used to separate likely members of the Tr14/16 clusters from the field star population. Several heavily reddened new members of the Tr14/16 association are identified, some of which may be at an earlier evolutionary stage compared to the visible cluster populations. The distribution of reddening material, deduced from background field star colour-excesses, is shown to closely agree with the distribution of neutral material indicated by the ^{12}CO observations of de Graauw *et al.* An examination of the reddening law for the nebula shows it to be clearly anomalous and characterized by a unique value of $R=A_V/E(B-V)=4.8$. This anomaly extends to all stars studied. An alternative interpretation of the reddening law is demonstrated by normalizing the colour-excess ratios with respect to $E(V-J)$ rather than $E(B-V)$. This shows normal extinction longward of 0.55μm (V) and reduced extinction shortward of this wavelength. Normal extinction in the infrared is also deduced from the $(J-H)$, $(H-K)$ diagram for the background field stars. It is suggested that a mechanism for grain destruction must be operating in the Carina nebula to explain this result.

1 Introduction

The Carina nebula (NGC 3372) is perhaps the best known H II region in the southern sky. In addition to the peculiar object η Carinae found in its midst, the nebula contains one of the highest concentrations of early O stars known in the Galaxy. As an illustration of this point, the two open clusters Trumpler 14 (Tr14) and Trumpler 16 (Tr16), located near the centre of the nebula, contain a total of 18 stars with spectral types between O3 and O7. Another prominent feature is a dark dust lane which cuts across the nebula in the vicinity of these clusters. Thus, conditions in

*Present address: Max-Planck-Institut für extraterrestrische Physik, 8046 Garching bei München, Federal Republic of Germany.

Carina provide a unique site for examining the effects of an intense radiation field on grains in the surrounding dust clouds.

The question of the association between the star clusters and the ionized gas of the nebula and the dust lane has long been a difficult one to answer. Radio observations such as the 2650 MHz map of Beard & Kerr (1966) show two distinct radio peaks located in the centre of the nebula. One, Carina II, is located roughly 3 arcmin north-west of the Tr16 cluster while the other, more intense peak, is located roughly 1 arcmin west of the Tr14 cluster. Although Carina II is coincident with an intense ionization region 1 arcmin north-west of η Carinae and the Tr16 cluster, Carina I has its peak in the dark lane to the west of Tr14. The presence of this radio peak and an associated far-infrared (80 μm) source argue for an interaction between the cluster Tr14 and the dust to power this emission (Harvey, Hoffmann & Campbell 1979). Perhaps the most convincing evidence for this interaction comes from the more recent work of de Graauw *et al.* (1981). Based on observations of the $^{12}CO(J=2\rightarrow 1)$ line, they suggest that a molecular cloud is partially wrapped around the optical nebula and obscures the region where Tr14 is interacting with the cloud. The overall picture presented by the far-infrared and ^{12}CO observations is one of an evolved H II region in which the clusters Tr14 and Tr16 are in the process of shedding the molecular cloud from which they formed.

The present investigation was aimed at determining the extent of the clusters Tr14 and Tr16 and the degree to which they are associated with the dust. Infrared surveys at 2.2 μm provide a means for obtaining a sample of the brightest members of the stellar population in the direction of these clusters. Subsequent *JHK* photometry combined with 2 μm low resolution spectra allows early type members of the open cluster populations to be distinguished from late type members of the field star population (e.g. Elias 1978; Jones *et al.* 1980). This allows obscured members of the cluster populations to be identified. A comparison with the result of Jones *et al.* (1981) indicates that the field star population detected by 2 μm scans should largely consist of late K and M giants. By using low resolution 2 μm spectra to estimate approximate spectral types on the basis of the 2.3 μm CO band depth, the colour-excesses of the field star sample provide an excellent indication of the density distribution in the nebula. This distribution provides a test of the model for the distribution proposed by de Graauw *et al.* (1981) based on ^{12}CO observations.

Having established a group of stars which are definitely members of the Tr14 and Tr16 clusters, the second aim of this investigation was to determine the nature of the reddening law at the centre of the nebula as precisely as possible. This is important because of the limits the reddening law can impose on the sizes and distributions of the grains responsible for the extinction. It is particularly important in Carina because there is ample evidence to show that the reddening law is anomalous for stars in the Tr14 and Tr16 clusters (e.g. Herbst 1976), although the true nature of this anomaly is not well understood. For example, it has been suggested that the strong radiation field from the O stars could be responsible for modifying the grain size distribution only in their immediate environment (e.g. Isobe 1971). It is therefore important to study stars deeply embedded in the nebula to determine if this anomalous extinction extends throughout the entire nebula.

2 Observations

Raster scans covering an 18×18 arcmin^2 area centred on RA $10^h 42^m 35^s.0$ and Dec. $-59° 24' 00''$ were made at 2.2 μm. This area includes the open clusters Tr14 and Tr16 and the positions of the two radio sources Carina I and Carina II. The scans were made with the Mount Stromlo Observatory (MSO) infrared photometer attached to the $f/15$ focus of the 3.9-m Anglo–Australian Telescope (AAT). The raster lines were spaced 10 arcsec apart, while the aperture diameter was 14 arcsec. Fig. 1 is an identification chart for the region showing the positions of all

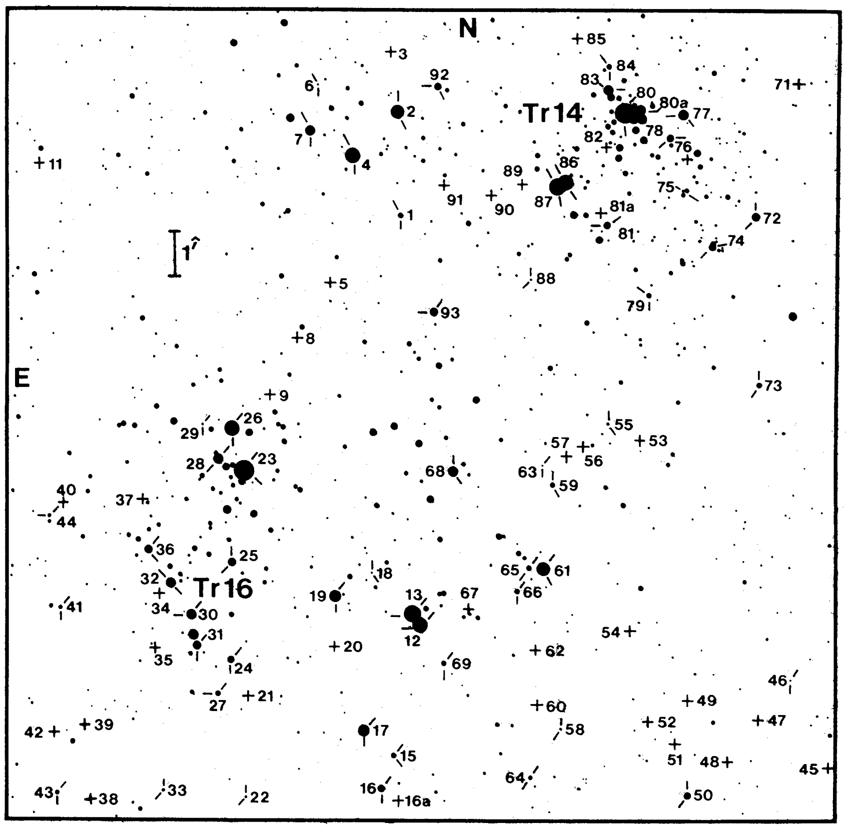

Figure 1. Identification chart for the region of the Carina nebula covered by the 2μm survey, based on a blue (IIa-O) photograph.

sources detected in these scans. The 1950.0 mean positions, magnitudes and colours of these sources are listed in Table 1.

Over a period from 1979 February to 1981 December, *JHK* photometry was obtained for 79 of the 93 sources detected in these scans. For those remaining, the positions and *K* magnitudes shown in Table 1 are as determined from the original scans. Photometry of the brightest sources was obtained using the MSO infrared photometer attached to the MSO 1.0-m telescope at Siding Spring Observatory. Additional photometry of the fainter sources was obtained with the Anglo–Australian Observatory infrared spectrometer–photometer (AAO IRSP) on the AAT. Many of the sources were observed more than once, allowing an estimate of the accuracy of the photometry. The maximum errors in the *K* magnitudes are ± 0.05 while the errors in the $J-H$ and $H-K$ colours are no more than ± 0.03. The AAO IRSP also has available a cooled circular variable filter-wheel which was used to obtain low resolution ($\lambda/\Delta\lambda \sim 50$) 2μm spectra of 32 sources. These sources were mostly selected for high reddening, on the basis of their observed colours or lack of a visible counterpart on a blue (IIa-O) plate of the region.

Although there are differences between the AAO and MSO photometric systems, both systems are well enough established that the transformations between them are well known (e.g. Jones & Hyland 1980; Allen & Cragg 1983). It has also become common practice to publish measurements obtained using the MSO systems, transformed to the AAO system. Thus, all measurements on the MSO system have been transformed to the AAO system using the following relation, from Jones & Hyland (1980):

$$(J-H)_{\mathrm{AAO}} = 1.07(J-H)_{\mathrm{MSO}}.$$

Table 1. Positions, magnitudes and colours for the Carina sources.

Source/Ident.[a]	RA (1950)	DEC	K	J-H	H-K	N[b]	CVF
IRS-01	10 42 39.5	-59 19 34	8.55	0.69	0.13	3	N
IRS-02/303311	10 42 39.8	-59 16 40	8.69	0.03	-0.04	1	N
IRS-03	10 42 41.1	-59 15 57	8.40	1.44	0.55	1	Y
IRS-04/93250	10 42 47.8	-59 18 08	6.72	0.10	0.03	4	N
IRS-05	10 42 51.7	-59 21 09	5.62	1.69	0.66	2	Y
IRS-06	10 42 54.8	-59 16 37	7.83	1.28	0.44	2	Y
IRS-07/93268	10 42 54.3	-59 17 40	8.98	0.05	0.00	1	N
IRS-08	10 42 56.8	-59 22 18	8.37	1.40	0.48	2	Y
IRS-09	10 43 05.1	-59 23 42	7.85	1.58	0.55	2	Y
IRS-11	10 43 41.3	-59 18 27	7.31	2.21	1.08	3	Y
IRS-12/93204	10 42 36.5	-59 28 44	7.90	0.07	0.04	1	N
IRS-13/93205	10 42 37.7	-59 28 30	7.29	0.07	0.01	1	N
IRS-15/16-21	10 42 41.0	-59 31 54	8.85	0.24	0.12	1	N
IRS-16/16-20	10 42 42.3	-59 32 42	9.97	-0.01	-0.03	1	N
IRS-16a	10 42 41.5	-59 32 50	9.32	2.36	0.99	1	Y
IRS-17/16-100	10 42 45.9	-59 31 09	7.60	0.15	0.08	2	N
IRS-18	10 42 44.9	-59 27 36	7.72	1.02	0.36	2	Y
IRS-19/16-104	10 42 51.2	-59 28 07	8.11	0.12	0.03	1	N
IRS-20	10 42 51.6	-59 29 13	7.98	1.73	0.73	3	Y
IRS-21	10 43 06.6	-59 30 24	9.01	1.35	0.50	2	N
IRS-22	10 43 06.8	-59 32 42	9.3	-	-	S	
IRS-23/η Car[c]	10 42 06.9	-59 25 16	1.15	1.12	1.36	1	N
IRS-24/16-23	10 43 09.8	-59 29 33	8.32	0.27	0.13	1	N
IRS-25/16-9	10 43 09.8	-59 27 21	8.79	0.14	0.04	1	N
IRS-26/303308	10 43 09.5	-59 24 20	7.65	0.09	0.03	2	N
IRS-27/16-22	10 43 11.9	-59 30 22	8.81	0.30	0.20	2	Y
IRS-28/16-1	10 43 12.1	-59 25 06	9.54	0.05	-0.05	1	N
IRS-29	10 43 14.8	-59 24 22	6.07	1.36	0.51	1	N
IRS-30/16-110	10 43 16.8	-59 28 34	7.76	0.26	0.10	2	Y
IRS-31/93343	10 43 16.7	-59 28 59	8.08	0.20	0.09	2	N
IRS-32/16-112	10 43 20.1	-59 27 49	7.95	0.21	0.12	1	N
IRS-33	10 43 20.6	-59 32 41	9.6	-	-	S	
IRS-34	10 43 22.0	-59 28 01	7.27	1.29	0.44	2	Y
IRS-35	10 43 24.6	-59 29 04	9.7	-	-	S	
IRS-36/16-115	10 43 24.6	-59 27 07	9.5	-	-	S	
IRS-37	10 43 24.6	-59 25 56	9.5	-	-	S	
IRS-38	10 43 33.7	-59 32 41	8.60	1.32	0.67	1	N
IRS-39	10 43 33.8	-59 31 07	9.4	-	-	S	
IRS-40	10 43 39.3	-59 26 05	7.71	1.33	0.48	2	N
IRS-41	10 43 40.0	-59 28 27	8.69	0.74	0.38	1	Y
IRS-42	10 43 40.0	-59 31 16	8.31	1.03	0.53	1	N
IRS-43/No. 15	10 43 39.7	-59 32 40	8.50	0.53	0.28	2	Y
IRS-44	10 43 41.7	-59 26 23	9.3	-	-	S	
IRS-45	10 41 24.2	-59 32 01	9.65	1.54	0.58	1	N
IRS-46	10 41 30.7	-59 29 57	6.49	1.20	0.39	2	Y
IRS-47	10 41 36.2	-59 30 50	7.23	1.69	0.65	2	N
IRS-48	10 41 41.4	-59 31 51	8.03	1.54	0.54	1	N
IRS-49	10 41 49.1	-59 30 28	8.33	1.82	0.72	1	Y
IRS-50/16-19	10 41 48.0	-59 32 30	8.50	0.17	0.06	2	N
IRS-51	10 41 51.3	-59 31 24	6.28	1.45	0.56	3	Y
IRS-52	10 41 55.9	-59 30 56	9.4	-	-	S	
IRS-53	10 41 57.2	-59 24 33	8.92	1.87	0.77	1	N
IRS-54	10 41 58.5	-59 28 53	9.3	-	-	S	
IRS-55	10 42 02.5	-59 24 13	9.5	-	-	S	
IRS-56	10 42 08.4	-59 24 46	8.66	1.78	0.71	2	Y
IRS-57	10 42 10.8	-59 24 55	9.22	1.33	0.47	3	Y
IRS-58	10 42 10.6	-59 31 07	10.02	0.53	0.04	1	N
IRS-59	10 42 13.0	-59 25 37	10.38	0.28	0.13	1	N
IRS-60	10 42 13.8	-59 30 36	8.84	0.93	0.57	1	Y
IRS-61/93162	10 42 14.3	-59 27 24	5.71	0.31	0.28	2	N

Table 1–*continued*

Source/Ident.a	RA	(1950)		DEC			K	J-H	H-K	Nb	CVF
IRS-62	10	42	15.7	-59	29	15	7.59	1.92	0.71	1	N
IRS-63	10	42	17.6	-59	25	20	10.44	1.03	0.48	1	N
IRS-64	10	42	16.3	-59	32	12	7.60	0.76	0.17	1	N
IRS-65/16-149	10	42	17.0	-59	27	20	6.99	0.51	0.33	1	N
IRS-66	10	42	19.1	-59	27	57	5.52	0.86	0.19	4	Y
IRS-67	10	42	28.4	-59	28	27	8.26	1.87	0.69	2	N
IRS-68/16-94	10	42	30.2	-59	25	17	9.3	-	-	S	
IRS-69	10	42	32.2	-59	29	39	7.76	0.56	0.10	2	Y
IRS-71	10	41	32.2	-59	16	57	9.02	3.64	1.67	2	Y
IRS-72/14-30	10	41	37.8	-59	19	27	8.34	0.25	0.11	1	N
IRS-73	10	41	36.3	-59	23	26	9.3	-	-	S	
IRS-74	10	41	44.9	-59	20	13	8.8	-	-	S	
IRS-75	10	41	50.4	-59	18	59	9.28	0.68	0.70	1	Y
IRS-76	10	41	50.5	-59	18	14	9.20	1.52	1.20	1	Y
IRS-77/14-20	10	41	50.2	-59	17	12	8.59	0.09	0.02	1	N
IRS-78/14-21	10	41	52.1	-59	17	40	9.27	0.23	0.11	1	N
IRS-79	10	41	53.8	-59	21	14	8.81	1.71	0.86	2	N
IRS-80/93129AB	10	42	02.2	-59	17	05	5.91	0.17	0.13	1	N
IRS-80a/93128	10	41	59.6	-59	17	05	-	-	-	S	
IRS-81/16-126	10	42	03.6	-59	19	44	9.14	0.25	0.16	1	N
IRS-81a	10	42	04.4	-59	19	38	8.35	2.39	1.15	2	Y
IRS-82	10	42	03.4	-59	17	51	7.27	2.56	1.14	3	Y
IRS-83/14-8	10	42	04.1	-59	16	44	8.16	0.16	0.14	1	N
IRS-84	10	42	03.5	-59	16	04	9.04	0.72	0.56	2	N
IRS-85	10	42	10.2	-59	15	34	8.23	2.75	1.28	1	N
IRS-86/93160	10	42	10.7	-59	18	44	7.09	0.10	0.05	1	N
IRS-87/93161AB	10	42	12.4	-59	18	48	6.95	0.10	0.06	1	N
IRS-88/No. 9	10	42	17.3	-59	21	02	3.93	1.57	0.59	2	Y
IRS-89	10	42	19.0	-59	18	50	6.10	1.84	0.79	1	N
IRS-90	10	42	23.5	-59	19	05	8.76	2.60	1.43	2	Y
IRS-91	10	42	31.5	-59	18	52	8.29	2.28	1.13	2	Y
IRS-92/16-35	10	42	33.9	-59	16	36	7.36	0.58	0.12	2	Y
IRS-93/16-10	10	42	34.3	-59	21	45	8.60	0.18	0.10	2	N

a All source identifications are as listed by Feinstein, Marraco, & Muzzio (1973) except for sources IRS-43 and IRS-88 which are from Forte & Orsatti (1981) and Blanco & Münch (1955) respectively.

b An "S" in the column showing number of observations indicates that no photometry was obtained for this object; the K magnitude listed is from the initial scan of the region and as such is only accurate to ± 0.1 magnitudes.

c Past observations of η Carinae (IRS-23) have shown it to be variable. The colours listed are the mean of five separate observations, the primary purpose being to estabish the mean colours.

As a check on the accuracy of the photometry, the J–H and H–K colours and the K magnitudes have been compared for the 11 stars in common with the studies of Thé, Bakker & Tjin A Djie (1980) and Thé & Groot (1983). Since the measurements by these two groups were obtained using the European Southern Observatory (ESO) photometric system, before comparison their observations were transformed to the AAO system using transformations from Wamstecker (1981) and Hyland, Jones & Mitchell (1982). The mean differences plus their standard deviations, in the sense Thé *et al.* or Thé & Groot minus this work, for J–H, H–K, and K are -0.01 ± 0.03, 0.01 ± 0.04, and -0.01 ± 0.08 respectively. The standard deviations are consistent with the accuracy of the data sets and the mean differences are much smaller than these standard deviations. Thus the photometry for the Carina sources presented here is consistent with previous work.

An examination of the K magnitude distribution for the measured sources indicates that the sample is complete down to a limiting K magnitude of $+9.0$. The only two exceptions in this sample are IRS-74 and IRS-80a whose measurements have been omitted from Table 1 because the photometry was contaminated by nearby stars.

3 CVF spectra and CO indices

3.1 DATA REDUCTION

Low-resolution ($\lambda/\Delta\lambda \sim 50$) CVF spectra were obtained for 32 of the sources detected in the survey of the Tr14/16 region of the Carina nebula. The majority of these sources were selected because they are heavily obscured, as indicated by an examination of a red (IV–N) plate of the survey area, provided by the UK Schmidt Telescope Unit (UKSTU) at Siding Spring Observatory. The remaining sources were selected as being representative of the various population groups as defined by their position in the $(J-H)$, $(H-K)$ diagram (see Fig. 3 and Section 4). These spectra are presented in Fig. 2 where individual spectra have been shifted vertically by an arbitrary amount.

The high atmospheric water vapour levels at the Siding Spring site on the nights of observation

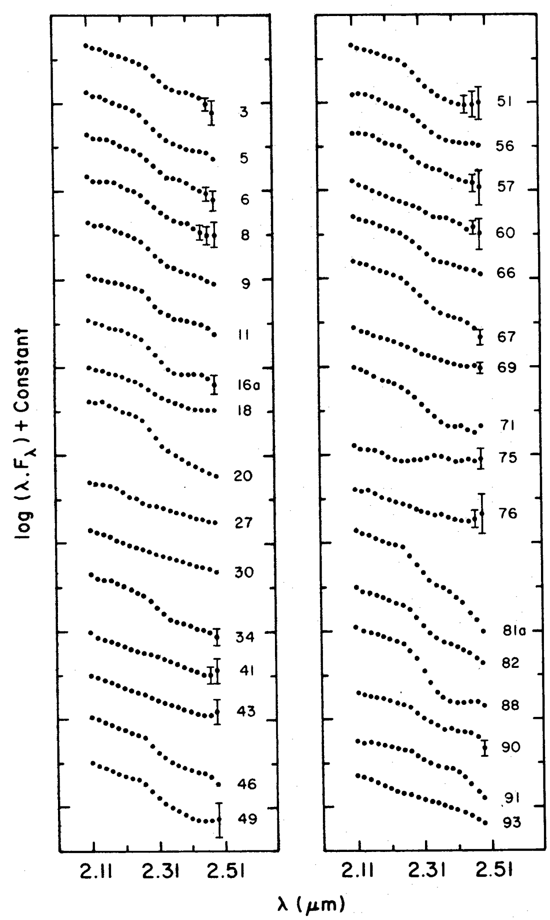

Figure 2. Low-resolution CVF spectra for a selection of the survey sources where the spectra have been shifted vertically by an arbitrary amount. Reddening corrections have been made for all spectra following the procedure outlined in the text.

required that the spectral range be restricted to 2.11 to 2.49 μm. With a step size of 0.02 μm over this range, the measured spectra consist of signal values at 20 points plus their associated errors. Since the CVF has an instrumental resolution of only 0.04 μm, this step size was necessary to fully sample the spectra. The instrumental effects were removed by normalizing the spectra with respect to HR 4114, an unreddened F0Ib star which is very close to the Carina nebula in both right ascension and declination (N.B. HR 4114 is not a photometric standard). No attempt was made to correct for the presence of a B_γ absorption feature in the standard because any such effect is likely to be very small at this resolution and there is no clear evidence for any observable feature at the B_γ position in the spectra of Fig. 2. In order to convert the observed spectra to fluxes, the spectrum of HR 4114 was assumed to follow the Rayleigh–Jeans approximation to a 7030 K blackbody. No atmospheric extinction corrections have been made to the spectra because of the close proximity of the standard to the Carina sources and because the standard was measured often enough during a night's observation that the maximum differential airmass was 0.05.

The spectra presented in Fig. 2 have been corrected for reddening by assuming a wavelength dependence of extinction of $\lambda^{-1.9}$ in the 1.2 to 3.5 μm spectral region. This value is taken from van de Hulst's theoretical curve No. 15, however similar results have been obtained from observational data (e.g. Landini *et al.* 1984). The magnitude of the reddening correction was based on a $H-K$ colour-excess determined by obtaining an approximate spectral type from the position of the star in the $(J-H)$, (H–K) diagram.

The principal purpose of taking CVF spectra of sources in the Carina nebula was to search for absorption due to the first overtone vibration–rotation band sequence of CO longward of 2.3 μm. At this resolution, individual band heads are not distinguishable; rather the overall effect is of one absorption band between 2.29 and 2.45 μm. From this absorption, a band-depth can be determined relative to what is assumed to be the continuum at 2.20 μm. Studies have shown that for stars later than ~G5 this band-depth provides an approximate indication of spectral type (e.g. Baldwin *et al.* 1973; Frogel *et al.* 1978). In order to quantify this band-depth versus spectral-type relation, Frogel, Persson, Aaronson & Matthews (1978; hereafter FPAM) have defined a 'CO Index' based on measurements of stars through a system of narrow-band filters with effective wavelengths of 2.20 and 2.36 μm; the effective wavelengths and half-power bandwidths having been chosen to sample the continuum and CO absorption bands without overlap. Using data from a large sample of stars they have determined mean CO indices for both dwarf and giant stars between spectral types G5 and M8.

Table 2 lists the CO indices that have been determined for the sources of Fig. 2 by convolving the spectral data with rectangular filter transmission functions having the same effective wavelengths and half-power bandwidths as FPAM. Tests with a wide range of filter transmission functions have shown that the shape has a negligible effect on the resulting CO indices as long as the same effective wavelengths and half-power bandwidth is used. The spectral types shown in Table 2 have been derived using the mean CO index versus spectral type relations determined by FPAM.

3.2 UNCERTAINTIES IN THE REDUCTION PROCEDURE

There are several uncertainties which can be introduced into the CO indices, and hence into the spectral types, through the reduction procedure described above. One such uncertainty lies in the adoption of a wavelength dependence of extinction of $\lambda^{-1.9}$ for dereddening the spectra. However, varying this value from $\lambda^{-1.9}$ to $\lambda^{-2.5}$ results in a change of only 0.03 mag in the CO index for the most heavily reddened source in the sample [IRS-71; $E(H-K)\sim1.5$]. This is equivalent to a change of only one or two subtypes when the CO index is converted to a spectral type.

Further uncertainty is introduced in the determination of a colour-excess, $E(H-K)$, to com-

Table 2. CO indices and spectral types.

Source	CO Index	Group[a]	Sp. type[b]
IRS-03	0.21	C	M3 III
IRS-05	0.27	C	M8 III
IRS-06	0.20	C	M2 III
IRS-08	0.20	C	M2 III
IRS-09	0.24	C	M6 III
IRS-11	0.22	D	M4 III
IRS-16a	0.30	D	M8 III
IRS-18	0.11	(F)	K2 III
IRS-20	0.35	C	M8 III
IRS-27	0.04	A	early
IRS-30	0.01	A	early
IRS-34	0.22	C	M4 III
IRS-41	0.03	B	early
IRS-43	0.05	B	early
IRS-46	0.22	C	M4 III
IRS-49	0.25	C	M7 III
IRS-51	0.30	C	M8 III
IRS-56	0.16	C	K5 III
IRS-57	0.18	C	M1 III
IRS-60	0.07	B	early
IRS-66	0.19	(F)	M2 III
IRS-67	0.29	C	M8 III
IRS-69	0.05	(F)	G8 III or K5 V
IRS-71	0.31	D	M8 III
IRS-75	-0.16	B	early
IRS-76	0.02	B	early
IRS-81	0.37	D	M8 III (+H_2O)
IRS-82	0.32	D	M8 III
IRS-88	0.51	C	M8 III (+H_2O)
IRS-90	0.15	D	K5 III
IRS-91	0.06	D	K0 III
IRS-93	0.02	A	early

[a] Sources are grouped according to their position in the (J-H),(H-K) diagram (see § 4). The (F) grouping is for foreground stars.

[b] For the purposes of classification, all late type stars are assumed to be of luminosity class III.

pute the magnitude of the reddening correction. For stars whose spectra showed evidence for a CO absorption feature, a mean spectral type of M3III was assumed. This follows from an application of the 2μm luminosity function developed by Jones *et al.* (1981), applied for the direction and distance of the Carina nebula (T. J. Jones, private communication). This amounts to a maximum uncertainty in $E(H-K)$ of ± 0.2 based on the intrinsic colours of FPAM (after transformation to the AAO photometric system using the relations given by Elias *et al.* 1983). The result is an uncertainty of ± 0.03 mag in the CO indices or one or two subtypes in the spectral types of the late type stars in the sample.

Similar arguments apply for the early type stars in the sample except that for those early type stars without spectral classification, a mean spectral type of 09V was assumed. However, except in a few cases, they are significantly less reddened than the late type stars. Hence this dereddening procedure has little effect on the appearance of their spectra. In addition, since their spectra show no evidence for CO absorption (see Fig. 2 and Section 4), no further quantitative information is required from them.

Although the Jones *et al.* (1981) 2μm luminosity function predicts that the majority of the field stars will be normal late type giants, it is also possible that there may be a small number of Mira-like late type giants in the sample. The spectra of these stars may be strongly affected by water vapour absorption bands, centred at 1.9 and 2.7μm, which are observable in the spectra of very cool stars (Hyland 1974). Both of these bands are sufficiently broadened at stellar temperatures to extend into the 2 μm window although an examination of published high-resolution spectra suggests that the 2.7 μm band is likely to have the most pronounced effect on the CO index. This will have the effect of increasing the measured CO index. Because it cannot be separated from the CO absorption however, the H_2O absorption adds an uncertainty that cannot be quantified without additional measurements.

In summary, changes in the adopted wavelength dependence of extinction of the magnitude discussed above and uncertainties in the determination of the colour excess, $E(H-K)$, result in spectral types derived from the CO indices which are uncertain by two or three subtypes, assuming that the majority of these stars are normal late type giants.

4 The nature of the sample

Fig. 3 is $(J-H)$, $(H-K)$ diagram for the sources in Table 1. Individual stars which are explicitly discussed in the text are identified by number. The straight lines labelled A and B provide an indication of the possible directions of reddening; line A has a slope of 2.09 (Jones & Hyland 1980) and line B has a slope of 1.96 (see Section 5). The curved lines show the intrinsic colours for a range of spectral types and luminosities. The line marked OB shows the intrinsic colours for

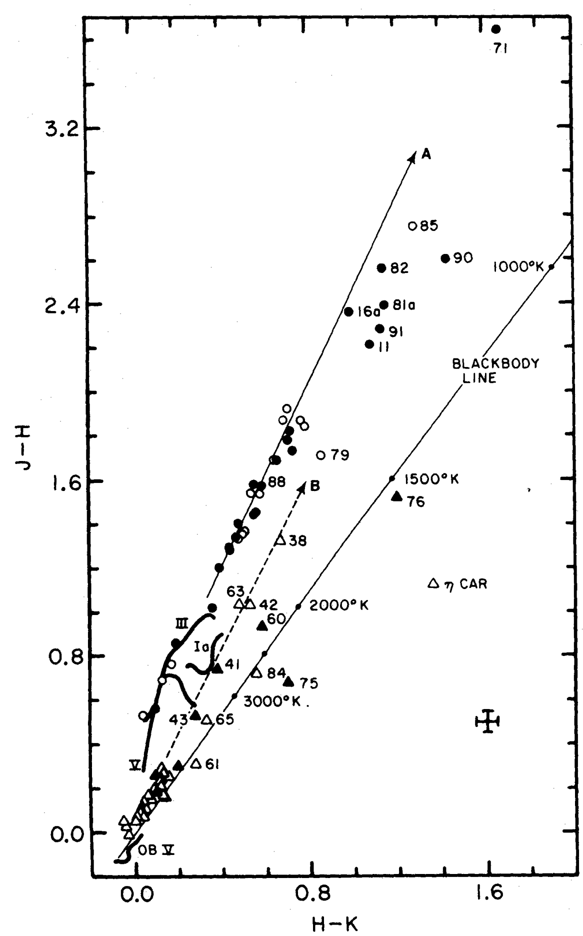

Figure 3. $(J-K)$, $(H-K)$ diagram for the Carina infrared sources. Stars considered probable field stars are represented by circles while likely members of the Tr14 or Tr16 clusters are represented by triangles. Filled symbols indicate those sources for which CVF spectra have been obtained. Lines A and B, which have slopes of 2.09 and 1.96 respectively, show possible reddening directions. Sources identified by number are discussed explicitly in the text.

main sequence stars earlier than A2 from Whittet & van Breda (1980). For late type stars the intrinsic colours for main sequence stars and giants with spectral types between G5 and M8 are from FPAM. For supergiants later than M0, the intrinsic colours of Lee (1970) were used. All intrinsic colours have been transformed to the AAO photometric system using relations from Hyland *et al.* (1982), Elias *et al.* (1983) and Elias, Frogel & Humphries (1985). Because of the diversity in the locations of the various groups of the stars in Fig. 3 it is convenient to define four general groups, designated A, B, C, and D, as follows.

4.1 THE GROUP 'A' STARS

In view of the large number of early O stars found in visible studies of the Tr14/16 region of the Carina nebula (e.g. Feinstein, Marraco & Muzzio 1973; hereafter FMM), a significant fraction of the sources detected in the 2 μm survey are expected to be O or early B stars. In addition, the distance of the Carina nebula, 2.7 kpc, corresponding to a distance modulus of 12.1 (FMM), is such that although supergiants with a wide range of spectral types may be detected in the 2 μm survey, the only normal main sequence stars likely to be detected are those earlier than B2. This is evident when the spectral types of those sources which can be identified with visible stars are examined. Accurate spectral classifications from Walborn (1973, 1982), Herbst (1976), and Levato & Malaroda (1982) plus the low dispersion objective prism work of Stephenson & Sanduleak (1971) and Lodén *et al.* (1976) indicate spectral types ranging from early B to early O, the majority being main sequence stars (see Table 3). Excluding two stars with very low reddening, IRS-07 and IRS-16, both of which are considered foreground stars by FMM on the basis of their $U-B$ and $B-V$ colours, the logical interpretation of the group of sources found in the lower left corner of Fig. 3 (i.e. those for which $J-H<0.35$ and $H-K<0.25$) is that they represent

Table 3. Colours for the Tr14/16 stars.

Source/Ident.	Sp.	Ref.[a]	U-V	B-V	V-R	V-I	V-J	V-H	V-K
IRS-02/303311	O5V	2	-0.73	0.13	0.29	0.38	0.38	0.41	0.36
IRS-04/93250	O3V((f))	1	-0.70	0.16	0.29	0.47	0.52	0.62	0.65
IRS-12/93204	O5V	1	-0.79	0.10	0.26	0.39	0.43	0.50	0.54
IRS-13/93205	O3V	1	-0.86	0.05	0.24	0.31	0.39	0.46	0.48
IRS-15/16-21			-0.07	0.47	0.67	1.20	1.72	1.96	2.08
IRS-17/16-100	O6V((f))	1	-0.57	0.21	0.36	0.65	0.79	0.94	1.02
IRS-19/16-104	O7V((f))	1	-0.65	0.14	0.19	0.35	0.53	0.64	0.68
IRS-24/16-23	O7Vn	2	-0.26	0.38	0.54	1.00	1.22	1.49	1.62
IRS-25/16-9	O9.5V	2	-0.48	0.23	0.34	0.70	0.79	0.93	0.98
IRS-26/303308	O3V((f))	1	-0.72	0.12	0.27	0.41	0.41	0.50	0.53
IRS-27/16-22			-0.11	0.49	0.58	1.16	1.69	2.00	2.20
IRS-30/16-110	O7V	2	-0.38	0.31	0.50	0.91	1.15	1.42	1.52
IRS-31/93343	O8Vn	2	-0.46	0.29	0.32	0.70	1.16	1.36	1.45
IRS-32/16-112	O4.5V((f))	2	-0.40	0.32	0.46	0.86	1.02	1.22	1.34
IRS-43	O4V	3	0.59	0.90	-	-	2.87	3.40	3.68
IRS-50/16-19	O9.5V	2	-0.32	0.33	0.42	0.80	1.03	1.21	1.29
IRS-65/16-149	O4ef	4	0.35	0.80	1.00	2.02	2.90	3.41	3.74
IRS-72/14-30			-0.03	0.50	-	-	1.39	1.64	1.75
IRS-77/14-20	O6V((f))	1	-0.45	0.28	0.47	0.72	0.91	1.00	1.02
IRS-78/14-21			-0.29	0.34	0.62	0.99	1.27	1.50	1.61
IRS-80/93129AB	O3If+O3V((f))	1	-0.62	0.16	0.32	0.56	0.76	0.93	1.06
IRS-81/16-126			-0.06	0.41	-	-	1.42	1.67	1.83
IRS-83/14-8	O6.5V((f))	1	-0.58	0.17	-	-	0.94	1.10	1.24
IRS-86/93160	O6III(f)	1	-0.60	0.17	0.33	0.50	0.58	0.68	0.73
IRS-87/93161AB	O6.5V((f))	1	-0.49	0.21	0.36	0.58	0.71	0.81	0.87
IRS-93/16-10	B0Vn	2	-0.39	0.30	0.41	0.79	0.95	1.13	1.23

[a] Spectral types are from (1) Walborn (1973, 1982); (2) Levato & Malaroda (1982); (3) Forte & Orsatti (1981); and (4) Thé et al. (1982), where only the first source is indicated.

the brightest members of the OB star population in the nebula. This well defined group is defined to be group A. In order to provide a comparison with other stars in the $(J-H)$, $(H-K)$ diagram, 2 μm spectra were obtained for three members of this group, shown as filled triangles in Fig. 3, all of which are essentially featureless, as expected for O or B stars (see Fig. 2 for spectra of sources IRS-27, IRS-30, and IRS-93).

4.2 THE GROUP 'B' STARS

Lines B in Fig. 3 shows an approximate reddening direction for the OB stars of group A [$E(J-H)/E(H-K)=1.96$, see Section 5]. Group B is defined to be those stars having $H-K>0.25$ which lie close to or to the right of this line. They are considered probable members of the Tr14/16 association although more heavily reddened than the majority of the cluster population. To confirm this, 2 μm spectra were measured for five of these stars; IRS-41, IRS-43, IRS-60, IRS-75 and IRS-76. No indication of a CO absorption feature is seen in any of these spectra although the spectrum of IRS-75 is clearly not featureless. Further evidence for the association of these stars with the Tr14/16 clusters may be found in the work of Thé *et al.* (1982). They have determined a spectral type for IRS-65 (16-149) of 04ef. Similarly, the source IRS-43 can be identified with star no. 15 in the work of Forte & Orsatti (1981) and which they classified O4V. This is consistent with the range in spectral types found for the brightest members of the Tr14/16 population. An additional argument against these being field stars is found in the study by Forte & Orsatti (1981) who conducted an objective prism survey for OB stars in the field of the Carina nebula. They found that roughly 80 per cent of these stars have spectral types later than B0. Since the survey described here was carried out at 2 μm, as pointed out in Section 4.1, at the distance of the Carina nebula the only normal main sequence stars likely to be detected are those with spectral types earlier than ~B2. Thus the very nature of the survey discriminates against the detection of early type stars in the field of the Carina nebula. Hence the group B stars most probably represent additional members of the Tr14/16 cluster populations, more deeply embedded in the nebula.

Several of the group B stars exhibit excess infrared emission, as indicated by their positions in Fig. 3, to the right of the normal direction of reddening and their proximity to the blackbody line. Two well-studied examples of this group are the WN7 star HD 93162 (IRS-61) and η Carinae (IRS-23). Both lie to the right of the normal reddening line and both are known to exhibit excess infrared emission. For the WN7 star this emission most likely arises in an extended photosphere while for η Carinae the emission is considered to be due to heated dust (Aitken & Jones 1975). This is consistent with the results of a study by Allen & Penston (1973) of the dust temperatures around hot stars. They concluded that the source of the small infrared excesses [$E(H-K)<0.4$] can be attributed to free–free emission from an extended photosphere while the larger excesses [$E(H-K)>0.4$] probably arise in heated dust.

Excluding η Carinae, the three objects with the largest excesses, IRS-75, IRS-76, and IRS-84 clearly require further study. Not just because they show indications of having excess infrared emission but also because all three are located very close to the Tr14 cluster. Why all three should be located near Tr14 is not clear, however there is evidence that Tr14 is embedded more deeply in the nebula and possibly at a different evolutionary stage compared to Tr16. The ^{12}CO observations of de Graauw *et al.* (1981) suggest that Tr14 is interacting more strongly with the molecular cloud surounding the Carina complex and is potentially younger than Tr16. If IRS-75, IRS-76 and IRS-84 are even more recently formed than the visible stellar population in Tr14 then it may be that these three stars have not yet been able to completely disperse the protostellar cloud from which they formed. In addition, the high reddening of these stars, assuming it is not all circumstellar, indicates that they lie on the far side of the Tr14 cluster; the side that is probably interacting with the molecular cloud. Adopting a scenario for sequential star formation such as suggested by Elmegreen & Lada (1977), the ionization front from the Tr14 O stars moving into the molecular cloud could have triggered new star formation. Thus these three stars may be at an earlier evolutionary stage compared to the visible Tr14 population.

4.3 GROUPS 'C' AND 'D'

Line A in Fig. 3 shows a possible reddening direction for late type giant stars, taken from the work of Jones & Hyland (1980) (see discussion in Section 5). The group of stars lying near this line occupy positions corresponding to normal reddened giants or supergiants and are therefore assumed to be members of the general field star population. An approximate spectral range for these stars may be estimated from a model for the 2μm luminosity function (Jones *et al.* 1981) applied for the distance and direction of the Carinae nebula (T. J. Jones, private communication). The model predicts the field star population to be mostly giants later than G8 with a mean spectral type of about M3III. To test this assumption, 2μm spectra have been obtained for roughly 60 per cent of these stars (see Fig. 2), all of which show evidence for a CO absorption feature, as expected for stars in this spectral range.

The group of stars lying near line A in Fig. 3, and for which $1.2<J-H<2.0$, are defined to be group C. In view of the distinct separation between the giant intrinsic colour sequence and the least heavily reddened member of this group, these stars are considered to define the general field star population seen behind the Carina nebula. Table 2 shows the spectral types derived from the spectra for a sample of these stars. The range in spectral types is in good agreement with the 2μm luminosity function of Jones *et al.* (1981). One star, IRS-88, shows a remarkably large value for the CO index of 0.50. This star can be identified with star no. 9 in the work of Blanco & Münch (1955) which they classify as type S on the basis of an objective prism spectrum. It has been further observed by Catchpole & Feast (1976) who confirm its classification as an S-type star. This classification is sufficient to explain the unusually high CO index since the CO bands are very deep in S stars compared to normal M giants (Merrill & Ridgway 1977).

Separate from the group C field stars but still considered members of the field star population are those stars in group D, which is defined to be stars for which $J-H>2.0$. The spectral types derived from the 2μm spectra (Table 2) confirm this classification in that they fall within the spectral range expected for normal late type field stars. This group is clearly separated by $E(J-H)\sim 0.3$ from the most highly reddened member of group C. This separation from the main body of field stars may be explained by the presence of an additional reddening component behind the Carina nebula. However, to explain why these stars all lie to the right of the normal reddening direction for late type giants it is necessary to consider a scenario where they either all suffer anomalous reddening or all have infrared excesses, or a combination of these. These points are discussed further in Section 5.

In addition to the reddened field stars there exists a small group of stars which lie close to the giant intrinsic colour sequence (the line marked III in Fig. 3). These stars are likely foreground objects since they are significantly less reddened than the general field star population. Although 2μm spectra have only been obtained for three of these stars, the spectral types derived from the spectra, in conjunction with their positions in the $(J-H)$, $(H-K)$ diagram, suggest this interpretation to be correct. This group also includes two stars in the lower-left corner of Fig. 3, IRS-07 and IRS-16, which are clearly early-type stars. They have been designated as foreground objects on the basis of their observed $U-B$ and $B-V$ colours by FMM. Note that in this context, the foreground classification only means that these stars are not behind and probably not embedded in the Carina nebula.

5 The reddening law for the Carina field stars

The work of Jones & Hyland (1980) on the reddening law for highly reddened field stars has shown that there is very little variation in the ratio $E(J-H)/(H-K)$ with direction. It is of interest then, to examine this ratio for the Carina field stars since a departure from normal would indicate a dust composition different to the general interstellar medium. Because no accurate spectral classifications exist for the Carina field stars, the method used to examine the reddening was to fit a straight line to the measured $J-H$, $H-K$ colours. This approach is valid because the differential reddening of these stars is much greater than any variation in the observed colours that might arise because of the range in spectral types present. In addition, the direction of normal reddening appears to be approximately along the giant intrinsic colour sequence, thus the errors involved in this approach are small.

In general, the observed colours of stars behind the Carina nebula will be influenced by three potentially different reddening components. First, a foreground component due to dust between the sun and the nebula; second, dust which is associated with the nebula; and third, dust behind the nebula. It is reasonable to assume that the foreground reddening component is the same for all background field stars because of the relatively small area being studied. A comparison of the colour-excesses of the most highly reddened members of the Tr14/16 clusters with the colour-excesses of the group C stars indicates it is also reasonable to assume that, at least to a first approximation, the reddening of the group C stars is primarily due to dust in the nebula. The group D stars are however, much more heavily reddened than those in group C and consequently their reddening may be partially due to material behind, but not necessarily associated with the Carina nebula. If this is true, the dust composition for this background material may not be the same as that associated with the nebula. As a result, two separate determinations of the reddening direction were made, one for only the group C stars and the other for all stars in groups C and D. The results of fitting straight lines to these two data sets are as follows:

group C (23 stars): $E(J-H)/E(H-K)=1.96\pm0.11$;
groups C and D (31 stars): $E(J-H)/E(H-K)=1.71\pm0.09$.

Note that the least squares fitting procedure used allows for equal errors in both $J-H$ and $H-K$.

Line A in Fig. 3 shows the reddening direction, $E(J-H)/E(H-K)$, from the work of Jones & Hyland (1980) and has a slope of 2.09 ± 0.10. Considering that the Jones & Hyland value was based on a fit to the upper envelope of a group of highly reddened stars, the result determined for the Carina group C stars is in good agreement. This is not unexpected since the Jones & Hyland result is a general one, based on observations of stars in a wide range of directions. Thus, assuming this reddening is largely due to dust in the nebula, the reddening law for the Carina nebula, at least in the infrared, must be considered to be normal.

The lower value of $E(J-H)/E(H-K)$ resulting from the inclusion of the group D stars can be explained if these stars are subject to reddening by dust which has a different composition compared to the dust associated with the Carina nebula. In fact, since these stars must also be reddened by dust in the nebula, the true value of $E(J-H)/E(H-K)$ would be even lower than 1.71. The existence of a background reddening component is clearly possible since observations in the direction of the Carina nebula are essentially looking into an appreciable length of the Sagittarius-Carina spiral arm (Georgelin & Georgelin 1976). An alternative explanation for this smaller value of $E(J-H)/E(H-K)$ is excess emission at $2\,\mu$m (K) which will increase $E(H-K)$ and thus lower the ratio $E(J-H)/E(H-K)$. A similar effect will be seen if there is a significant fraction of supergiants in the sample. Considering that most of the group D stars are found in the immediate vicinity of the Tr14 cluster, both of these explanations are unlikely to be true. The probability of finding a group of supergiants or late type giants with excess emission confined to this small a region is extremely low. Thus, the most likely explanation for the lower value of $E(J-H)E(H-K)$ found for the group D stars is that they suffer extinction by dust behind the Carina nebula but this dust has a different composition compared to that associated with the nebula.

6 The distribution of reddening material in the nebula

The infrared colour-excess $E(J-K)$ is directly proportional to the dust column density in the line-of-sight providing the composition of the dust remains the same over the area considered (e.g. Jones *et al.* 1980). This colour-excess can be converted to total visual absorption A_V using the relation $A_V=6.0\ E(J-K)$ which is derived from the work of Schultz & Wiemer (1975) and which represents a normal reddening law. Thus, by using the colour-excesses of late type field stars located behind the Carina nebula, after subtracting the foreground reddening component, the distribution of reddening material in the nebula can be examined.

The foreground component was estimated from the colour-excesses of the least heavily reddened O stars in the Tr14/16 clusters. Taking the seven stars with the smallest colour-excesses results in an upper limit for the foreground reddening of $E(J-K)=0.30\pm0.07$ ($A_V\sim1.8$), in reasonable agreement with the expected extinction in the galactic plane. For the background field stars $E(J-K)$ was computed using the intrinsic colours of FPAM (after transformation to the AAO photometric system using the relations given by Elias *et al.* 1983) and the spectral types determined from the CVF spectra (Table 2). For those stars for which no spectra were obtained, a mean spectral type of M3III was assumed. Because only an approximate indication of the distribution of reddening material is required, the assumption of a mean spectral type is not an unreasonable one. Similarly, variations in the relationship between A_V and $E(J-K)$ by as much as 30 per cent will not alter the conclusions of this work. Additional uncertainty is introduced however, through the assumption that the reddening of the field starts is entirely due to material in or near the nebula. Also, the distribution of field stars is very irregular. Thus the resulting

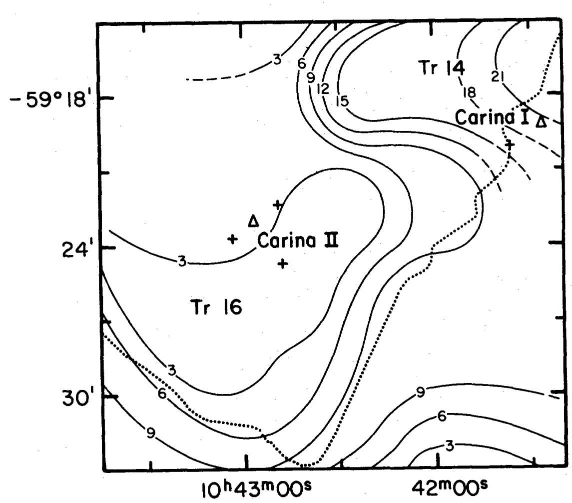

Figure 4. Approximate distribution of visual absorption A_V over the survey area derived from colour-excesses of background field stars. A foreground absorption of $A_V\sim1.8$ mag exists in addition to that shown here. The positions of the two radio sources, Carina I and II, are indicated by crosses. Note that the three crosses shown near Carina II represent three distinct peaks resolved by Retallack (1978) at 1415 MHz. The position of the far-infrared (80 μm) peaks associated with these sources are indicated by triangles. The dashed line indicates the approximate boundary between ionization and absorption.

density distribution should be considered only as indicative of the maximum amount of absorbing material in a particular region.

Fig. 4 shows a plot of the distribution in A_V in the direction of the Carina nebula, as determined from the field stars behind the nebula. The two radio sources Carina I and II are shown represented by crosses in Fig. 4 (Retallack 1978). Note that the three crosses shown near Carina II represent three distinct peaks resolved by Retallack. Open triangles indicate the positions of the far-infrared (80 μm) peaks apparently associated with these sources (Harvey *et al.* 1979). So that the A_V isophotes can be compared with the position of the dust lane, the approximate boundary between ionization and dust is shown by a broken line. Two points immediately arise from this comparison:

(i) The contours follow the dark lane across the south-west corner of the survey area, and curve around and across to the south-east corner. The presence of several heavily reddened early type stars in the south-east corner suggests that the absorbing material is actually in front of the Tr16 cluster at this point. An examination of the colour-excesses of the early type stars in the south of Tr16 shows a distinct increase in extinction towards the southern edge. Also in good agreement with this view is the increase in the $E(B-V)$ colour-excess seen by FMM, to the south and south-east.

(ii) The absorbing material continues to the north-west and north but here it must be behind the Tr14 cluster since the brightest members of this cluster only show close to the foreground reddening component. If any of the heavily reddened early type stars (group B) seen in this region are associated with the Tr14 cluster, they must either be on the far side of the Tr14 cluster or suffer large amounts of circumstellar reddening (see discussion in Section 4).

This result is in good agreement with the distribution of neutral material shown by the ^{12}CO($J=2\rightarrow 1$) observations of de Graauw *et al.* (1981). They find a neutral cloud in front of the south and south-east portion of the Tr16 ionization region, the highest density being in the south-east corner. In the north and north-west their observations indicate most of the neutral material is located behind the Tr14 cluster. The picture of the Tr14 cluster and the Carina I radio source that evolves from the ^{12}CO observations of de Graauw *et al.* (1981) and the far-infrared observations of Harvey *et al.* (1979) is one of the O stars on the Tr14 cluster interacting with the molecular cloud where, moving progressively further west, first the radio peak and then the far-infrared peak is seen. de Graauw *et al.* also suggest that this neutral cloud is partially wrapped around the Tr14 ionization region and is responsible for obscuring the interface between ionized and neutral material which is producing the far-infrared emission. For the Tr16 cluster and the Carina II radio source, the lower A_V values seen in the vicinity of Carina II are also in good agreement with the ^{12}CO and far-infrared observations. Here, the picture is one of a lower density dust cloud heated by the surrounding O stars, but optically thin to the heating flux from the O stars. A consequence of this is the lower far-infrared surface brightness compared to Carina I and the presence of only weak ^{12}CO emission.

One further point which relates to the distribution of reddening material arises when one considers the distinct separation of the background field stars into two groups (i.e. groups C and D). In fact, all but two of the more heavily reddened group (group D) lie in the immediate vicinity of the Tr14 cluster. If this were due to a local density enhancement in the neutral cloud wrapped around the Carina nebula, one might expect a more continuous distribution in the field star colour-excesses. Since this is not seen, the presence of another reddening component behind the nebula becomes more likely. In addition, while both the ^{12}CO observations of de Graauw *et al.* (1981) and the A_V distribution derived by Dickel (1974) (from 5000 MHz and Hα observations) show a slight density increase in the region of the Carina I radio peak, nothing is seen at the position of the Tr14 cluster which indicates absorption of the magnitude seen in Fig. 4. Thus the observational evidence points to an additional reddening component behind the Tr14 cluster.

7 The reddening law for the Tr14/16 OB stars

It has long been suspected that in the vicinity of the hot OB stars the interstellar reddening law may be modified due to the influence of the strong radiation field on the dust grains responsible for the extinction. With the large number of O stars found in the Tr14/16 region of the Carina nebula an ideal site is available for examining this proposition. The weight of evidence indicates that the reddening law for the Tr14/16 OB stars is anomalous. Both FMM and Herbst (1976) have shown that the ratio $E(V-I)/E(B-V)$ for some stars in the clusters Tr14 and Tr16 is appreciably higher than the normal interstellar value. This extinction anomaly was confirmed by Forte (1978) on the basis of new RI photometry for a large sample of stars in these clusters. More recently Turner & Moffat (1980) obtained a relatively normal value for the ratio of total-to-selective extinction, $R=3.20\pm0.28$, for the entire Carina nebula based on a variable extinction study of likely members of the Tr14, Tr16 and Cr228 clusters. Essentially Turner & Moffat reconcile their result with prior reddening law investigations by suggesting there may be significant anomalies in the *RI* photometry of both Herbst (1976) and Forte (1978). Thé *et al.* (1980) have obtained *VRIJHKLM* photometry for the eight brightest O stars in Tr14 and Tr16 clusters. Using the colour difference method, they find that the extinction law in the directions of their selected stars are without exception anomalous; characterized by a mean R value of 3.9 ± 0.1. Thé & Groot (1983) have added three more Tr16 stars to this work, with exactly the same conclusions. These two studies represent the first attempts to extend the reddening law investigations to longer wavelengths, a necessity if the true form of the reddening law is to be understood. Unfortunately, because the majority of these stars are the brightest O stars in the Tr14 and Tr16 clusters, one possible interpretation of these results is that the reddening law is only anomalous in the immediate vicinity of these stars. This proposal can now be tested with the additional OB stars identified in Section 4 which allow the reddening law to be examined for a group of stars with a much greater range in reddening, distributed over a much larger portion of the Carina nebula.

The approach adopted for examining the reddening law was to select stars for which accurate spectral classifications were available and determine reddening directions from the colour-excess diagrams. An alternative approach was used by Schultz & Wiemer (1975) who determined reddening directions from colour–colour diagrams for stars of similar spectral type. As long as the data set is restricted to stars for which the variation in intrinsic colours is much smaller than the variation in the observed colours due to reddening, this approach is valid. In fact, because the variation in intrinsic colours of O and early B stars is small, this approach may also be applied for the OB stars in Carina.

There are 26 stars in the infrared sample which can be identified with visible stars and which, on the basis of their positions in the $(J-H)$, $(H-K)$ diagram, are members of the Tr14/16 association. Of these 26 stars, 20 have accurate spectral classifications available. The identifications, colours and spectral types for these stars are presented in Table 3. All identifications are from FMM, with the exception of IRS-43 which was identified with star no. 15 of Forte & Orsatti (1981). Spectral types are taken from the work of Walborn (1973, 1982), Levato & Malaroda (1982), Forte & Orsatti (1981), and Thé *et al.* (1982). In calculating the colours, the *UB* data of FMM was used almost exclusively, this being by far the most extensive work on the Carina nebula. The one exception to this was IRS-43 for which the *UBV* data was taken from Forte & Orsatti (1981). The *VRI* data is a mean of the results of FMM, Forte (1978), Thé *et al.* (1980), Thé & Groot (1983), and Feinstein (1982), where data exists in common between any of these groups. This use of data from several sources was necessary to obtain a statistically significant data set. In addition, because small differences exist between the *RI* photometry of the various groups, averaging the results provided the most reasonable estimate of the true magnitudes as no evidence was available to indicate which set of photometry was more reliable.

As near as can be determined, all of the published *UBVRI* photometry is on the Johnson photometric system (Johnson *et al.* 1966), with the exception of the *RI* data of Feinstein (1982) which is on the Cousins photometric system. Before combining the data sets, the Feinstein (1982) *RI* data was transformed to the Johnson system using transformation given by Bessell (1979). Colour-excesses were then calculated for the 20 stars for which spectral types were available, using the intrinsic colours of Johnson (1966) for $\lambda<1\,\mu$m and Whittet & van Breda (1980) for $\lambda>1\,\mu$m. These values are presented in Table 4.

7.1 THE COLOUR-EXCESS DIAGRAMS AND REDDENING DIRECTIONS

The data of Table 4 was used to plot the colour-excess diagrams shown in Fig. 5. The solid line in each diagram represents the line of best fit to the data points. The dashed lines show the reddening directions from a mean reddening law, as discussed below. The reddening directions determined from these colour-excess diagrams are presented in Table 5 in the form of colour-excess ratios. For comparison, the colour-excess ratios from curve no. 15 of van de Hulst (see Johnson 1968) and those for a mean reddening law are also presented. The sources of this mean law are as follows: the ratio $E(V-K)/E(B-V)$ is an average of the results of Schultz and Wiemer (1975) and Barlow & Cohen (1977), $E(V-H)/E(B-V)$ is taken from Jones & Hyland (1980), and $E(V-J)/E(B-V)$, $E(V-I)/E(B-V)$, and $E(V-R)/E(B-V)$ are taken from Schultz & Wiemer (1975). Table 5 also shows the reddening directions determined from an analysis of the colour–colour diagrams for the 26 stars for which visible identifications exist. This is useful because this sample contains several more highly reddened stars. Some additional scatter might be expected in these values because of the range in spectral types present. However, relative to the range in reddening seen from the colour-excesses, this will not significantly affect the results. Finally, it is important to note that the presence of the two very highly reddened stars in the colour-excess diagrams does not appreciably alter the fitted slopes except for the $E(V-H)/E(B-V)$ and

Table 4. Colour-excesses for the Tr14/16 stars.

Source/Ident.	E(U-V)	E(B-V)	E(V-R)	E(V-I)	E(V-J)	E(V-H)	E(V-K)
IRS-02/303311	0.73	0.45	0.44	0.85	1.07	1.23	1.28
IRS-04/93250	0.76	0.48	0.44	0.94	1.21	1.44	1.57
IRS-12/93204	0.68	0.42	0.41	0.86	1.12	1.32	1.46
IRS-13/93205	0.60	0.37	0.39	0.78	1.08	1.28	1.40
IRS-17/16-100	0.89	0.53	0.51	1.12	1.48	1.76	1.94
IRS-19/16-104	0.81	0.46	0.34	0.82	1.22	1.46	1.60
IRS-24/16-23	1.20	0.70	0.69	1.47	1.91	2.31	2.54
IRS-25/16-9	0.92	0.53	0.48	1.16	1.43	1.70	1.84
IRS-26/303308	0.74	0.44	0.42	0.88	1.10	1.32	1.45
IRS-30/16-110	1.08	0.63	0.65	1.38	1.84	2.24	2.44
IRS-31/93343	0.98	0.60	0.47	1.17	1.85	2.18	2.37
IRS-32/16-112	1.06	0.64	0.61	1.33	1.71	2.04	2.26
IRS-43	2.05	1.22	-	-	3.56	4.22	4.60
IRS-50/16-19	1.08	0.63	0.56	1.26	1.67	1.98	2.15
IRS-65/16-149	1.81	1.12	1.15	2.49	3.59	4.23	4.66
IRS-77/14-20	1.01	0.60	0.62	1.19	1.60	1.82	1.94
IRS-80/93129AB	0.84	0.48	0.47	1.03	1.45	1.75	1.98
IRS-83/14-8	0.88	0.49	-	-	1.63	1.92	2.16
IRS-86/93160	0.86	0.49	0.48	0.97	1.27	1.50	1.65
IRS-87/93161AB	0.97	0.53	0.51	1.05	1.40	1.63	1.79
IRS-93/16-10	0.99	0.60	0.54	1.21	1.57	1.89	2.07

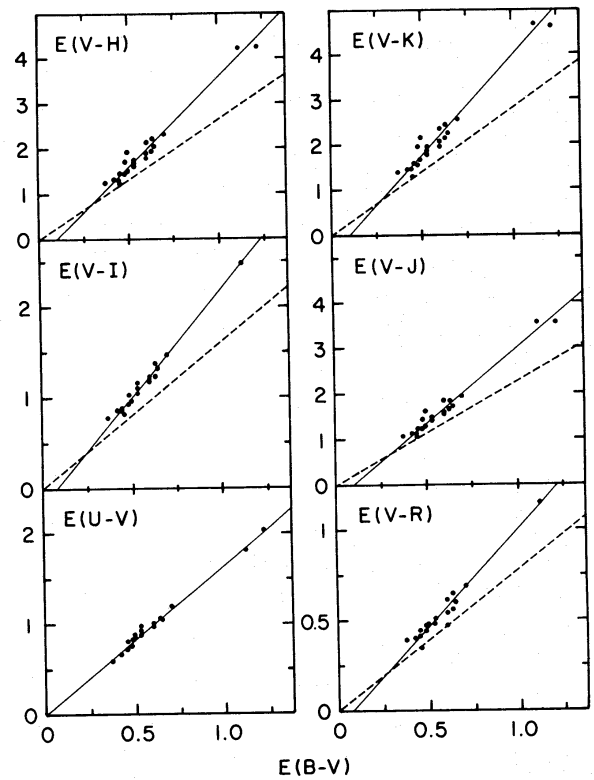

Figure 5. Colour-excess diagrams for the Tr14/16 OB stars based on the data presented in Table 4. The solid line in each diagram shows the result of an unconstrained least-squares fit to the data points. For comparison, the dashed lines show the reddening directions characteristic of a normal reddening law. Note that in the $E(U-V)$, $E(B-V)$ diagram, the solid and dashed lines are essentially coincident.

$E(V-K)/E(B-V)$ diagrams. In these two cases however, the removal of these stars results in slightly higher slopes, a result which does not alter the conclusions presented here.

A comparison of the colour-excess ratios derived for the Tr14/16 OB stars with those from a normal reddening law, as shown in Table 5, clearly indicates that in this region the reddening law is anomalous. It is not possible to account for the higher than normal colour-excess ratios in terms of excess infrared emission because the positions of all these stars in the $(J-H)$, $(H-K)$ diagram shows no indication of any significant infrared excesses. This would also require that the more heavily reddened stars have the largest excesses; there is no evidence to support this proposition. In addition, in the study of Of and Oe stars by Barlow & Cohen (1977), they find that while excess free–free emission is common at 3.6μm it is only sometimes detectable at 2.2μm. An alternative proposal is that the photometry may be contaminated by nebular emission but measurements of several of the brightest O stars in the nebula using different aperture sizes showed no differences greater than the quoted photometric errors.

One potential problem lies in the combination of data obtained with different photometric systems. In particular, the infrared data (i.e. *JHK*) is combined with the *UBV* photometry of FMM and the *RI* photometry of a number of groups (including FMM) in order to derive the reddening law. However, comparisons of the data sets suggests good agreement between the measured *UBV* data (e.g. Turner & Moffat 1980; Feinstein 1982) and the *VRI* data (Thé *et al.* 1980). The good agreement between the reddening directions determined from the colour–colour diagrams and the colour-excess diagrams shows both the lack of dependence on the intrinsic colours and the homogeneity, in terms of spectral type, of the data set. Finally, to consider the

Table 5. The reddening law for the TR14/16 stars.

Data source	E(U-V)/E(B-V)	E(V-R)/E(B-V)	E(V-I)/E(B-V)	E(V-J)/E(B-V)	E(V-H)/E(B-V)	E(V-K)/E(B-V)
van de Hulst curve No. 15	-1.71	0.80	1.62	2.30	2.58	2.78
Mean law		0.78	1.60	2.23	2.62	2.79
Colour-excess diagrams	-1.65 (±0.04)	1.09 (±0.12)	2.37 (±0.05)	3.32 (±0.05)	3.94 (±0.05)	4.34 (±0.05)
Colour-colour diagrams[a]	-1.70 (±0.06)	1.10 (±0.15)	2.34 (±0.05)	3.30 (±0.06)	3.90 (±0.05)	4.31 (±0.05)
Colour-colour diagrams[b]				3.38 (±0.06)		4.36 (±0.05)
Colour-colour diagrams[c]				3.41 (±0.06)		4.31 (±0.05)

[a] JHK photometry on the AAO photometric system.

[b] Determined after the J and K data in Table 3 had been transformed to the Johnson photometric system.

[c] Determined after the J and K data in Table 3 had been transformed to the CIT photometric system.

dependence of the results on the infrared photometric system used, the ratios $E(V-J)/E(B-V)$ and $E(V-K)/E(B-V)$ were determined from colour–colour plots after the $V-J$ and $V-K$ colours of Table 3 had been transformed to both the Johnson and CIT systems (using transformations from Elias *et al.* 1985). As shown in Table 5, the changes in the derived reddening slopes are small. Thus, comparison of the reddening law derived from results obtained on the AAO photometric system with the mean reddening law and van de Hulst curve no. 15 is an acceptable measure of whether or not an anomaly exists. In conclusion therefore, the reddening law in the centre of the Carina nebula is abnormal, as illustrated in Table 5.

In order to make a comparison with previous results, a value of the ratio of total-to-selective extinction, $R=A_V/E(B-V)$, may be obtained from the data of Table 5 by extrapolating the resulting extinction curve to longer wavelengths. The value thus obtained is $R=4.7\pm0.1$. The actual value for R may be higher because of the absence of any data for wavelengths longer than $2.2\,\mu$m. Whittet & van Breda (1980) however, suggest that the approximation $R=1.1\ E(V-K)/E(B-V)$ which is commonly used to deduce R in the absence of complete long wavelength data, is relatively insensitive to the adopted reddening law. Using this approximation with the slope determined from the $E(V-K)$, $E(B-V)$ diagram results in a value of $R=4.8$. This is in excellent agreement with the result of Herbst (1976) for the general direction of the Tr14, Tr16, and Cr228 clusters of $R=4.7\pm0.5$, obtained by the variable extinction method. Also in good agreement with this result is the value of 4.3 obtained by Forte (1978) for the Tr14 and Tr16 stars based on $V-R$ and $V-I$ colour-excesses. Thé *et al.* (1980), on the other hand, find a slightly lower value of 3.9 ± 0.1. This lower value may be a consequence of the different method used or perhaps a result of considering only the brightest visible stars in the nebula and hence only a relatively small range in reddening.

The most important result of this study is that the reddening law is anomalous for all stars in the sample. This includes stars with a large range of reddening, widely distributed within the nebula. An examination of the distribution of the OB stars indicates that the majority of the more heavily

Table 6. An alternative representation of the reddening law.

Data source	E(U-V)/E(V-J)	E(B-V)/E(V-J)	E(V-R)/E(V-J)	E(V-I)/E(V-J)	E(V-H)/E(V-J)	E(V-K)/E(V-J)
van de Hulst curve No. 15	-0.74	-0.43	0.35	0.70	1.12	1.21
Mean law		-0.45	0.35	0.72	1.17	1.25
Colour-excess diagrams	-0.49 (±0.09)	-0.30 (±0.05)	0.30 (±0.08)	0.67 (±0.08)	1.18 (±0.02)	1.30 (±0.03)
Colour-colour diagrams	-0.51 (±0.11)	-0.30 (±0.06)	0.30 (±0.09)	0.66 (±0.07)	1.18 (±0.02)	1.30 (±0.03)

reddened stars are found to the south and south-east of Tr16. In contrast, the only heavily reddened stars in the Tr14 region exhibit excess emission and their exact nature is uncertain. This is consistent with the view presented in Section 6 where a neutral cloud is seen in front of the southern portion of Tr16 but lies behind the Tr14 cluster. More importantly, it also indicates that the material in the neutral cloud must also conform to this reddening law.

7.2 THE IMPLICATIONS OF THE REDDENING LAW

The large value of R implies a grain size distribution biased towards larger than normal sized particles. One way the grain size distribution could be altered is by grain growth through accretion, a mechanism proposed to account for the presence of larger grains in dense, low temperature regions. However, this seems unlikely in the hostile environment which the large concentration of O stars in the Tr14/16 regions represents. A more plausible mechanism is the destruction of grains responsible for the visible extinction, resulting in reduced values of $E(B-V)$.

If the $E(B-V)$ colour-excesses (and colours) for the Tr14/16 OB stars are anomalously low then the reddening law in the nebula may be better represented by considering the colour-excess ratios determined relative to some other wavelength range. To examine this possibility the data of Table 4 was used to determine the colour-excess ratios at all wavelengths relative to $E(V-J)$. J was chosen because it will most closely represent emission from the stellar photosphere and be least affected by excess emission. The results of this exercise are presented in Table 6. Also included in this table are the values determined from curve no. 15 of van de Hulst (see Johnson 1968) and those for a mean reddening law, as discussed above. Reddening directions were also

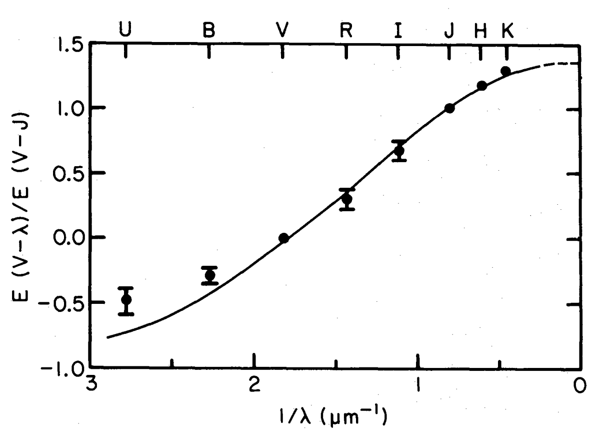

Figure 6. The reddening law for the Tr14/16 OB stars (filled circles) normalized to $E(V-J)=1.0$. The solid line represents a normal reddening law, as discussed in the text.

determined from the colour–colour diagrams for the 26 stars for which visible identifications are available. To illustrate this form of the reddening law for the Tr14/16 OB stars more clearly, Fig. 6 shows a plot of $E(V-\lambda)/E(V-J)$ versus $1/\lambda$ in which the results for the Tr14/16 stars are shown as filled circles and the mean interstellar reddening law is shown as a solid line. The diagram clearly indicates, within the calculated errors, that for wavelengths beyond $0.55\,\mu$m (V) the reddening law is very close to normal. Such a result is not unexpected since the ratio $E(J-H)/E(H-K)$ derived from the background field stars is also very close to normal. This provides further support for the argument that a mechanism for grain destruction may be operating in the Carina nebula, resulting in an anomalous grain size distribution and hence an anomalous value of $R=A_V/E(B-V)$ where the anomaly is due to reduced extinction in the U and B bandpasses. Note that this also requires the extinction in the U and B bandpasses to be close to grey, to explain the relatively normal value found for the ratio $E(U-V)/E(B-V)$.

8 Conclusions

This study effectively demonstrates the value of *JHK* photometry combined with low resolution spectrophotometry in the study of stellar complexes associated with nebulosity. The following conclusions can be drawn from the results of this study:

(i) A group of heavily reddened stars (i.e. relative to the visible stellar population) has been identified as being likely members of the Tr16 and Tr14 clusters. In the case of Tr16 these stars lie on the periphery of the visible cluster and their high reddening is largely a consequence of overlying absorption. This absorption is evident from both the distribution of reddening material deduced from the field star colour-excesses and the distribution of neutral material determined from the ^{12}CO observations of de Graauw *et al.* (1981). For Tr14, the only heavily reddened early type stars are located inside the boundaries of the visible cluster. In addition, all three of these heavily reddened stars exhibit excess $2\,\mu$m emission. It is suggested that these stars could have formed as a result of an ionization front from the Tr14 OB stars moving into the molecular cloud behind the Tr14 cluster. The excess emission could then be explained in terms of thermal emission from the remnants of the protostellar clouds from which these stars formed. Note that these stars must still be well evolved since no compact far-infrared sources are detected near Tr14.

(ii) The distribution of absorption throughout the nebula as determined from the colour-excesses of background field stars shows good agreement with the distribution of neutral material indicated by the ^{12}CO observations of de Graauw *et al.* (1981). However, because the spatial distribution of these field stars is irregular and because these stars may also be reddened by material behind the nebula, the derived absorption distribution should be treated as only indicative of the maximum amount of absorption in any particular region. On a larger scale, the results are sufficient to show that the absorption is largely in front of the southern portion of the Tr16 cluster and behind the Tr14 cluster. There is also evidence to suggest that an additional reddening component exists behind the Tr14 cluster. However, the irregular field star distribution and the relatively small number of stars involved make this difficult to confirm.

(iii) A study of the Tr14/16 OB stars shows the reddening law to be anomalous for all stars in the sample, characterized by a unique value of the ratio of total-to-selective extinction, R=4.8. This is interpreted in terms of a grain size distribution biased towards larger than normal sized particles. Considering the reddening law normalized with respect to a wavelength range other than $E(B-V)$ has provided an additional insight into this anomalous reddening. In this case normalization with respect to $E(V-J)$ leads to the conclusion that the extinction anomaly affects only the extinction in the U and B bandpasses. This provides strong constraints on models of the grain size distribution within the Carina nebula.

Acknowledgments

I am most grateful to Professor J. A. Thomas for his continued support and encouragement: Drs T. J. Jones, A. R. Hyland and A. T. Tokunaga for their advice and helpful discussions; Kris Sellgren for a critical reading of the manuscript; the MSO and AAT time allocation committees for allocation of time on their respective telescopes; Mike Barnett for providing a plate of the Carina nebula; and the UK Schmidt Telescope Unit for providing prints of several plates of the Carina nebula. I acknowledge the support of an Australian Commonwealth postgraduate research award during the period when the observations for this work were carried out.

References

Aitken, D. K. & Jones, B., 1975. *Mon. Not. R. astr. Soc.,* **172,** 141.
Allen, D. A. & Cragg, T. A., 1983. *Mon. Not. R. astr. Soc.,* **203,** 777.
Allen, D. A. & Penston, M. V., 1973. *Mon. Not. R. astr. Soc.,* **165,** 121.
Baldwin, J. R., Frogel, J. A. & Persson, S. E., 1973. *Astrophys. J.,* **184,** 427.
Barlow, M. J. & Cohen, M., 1977. *Astrophys. J.,* **213,** 737.
Beard, M. & Kerr, F. J., 1966. *Aust. J. Phys.,* **19,** 875.
Bessell, M. S., 1979. *Publs astr. Soc. Pacif.,* **91,** 589.
Blanco, V. M. & Münch, L., 1955. *Bol. Obs. Ton. Tac.,* **12,** 17.
Catchpole, R. M. & Feast, M. W., 1976. *Mon. Not. R. astr. Soc.,* **175,** 501.
de Graauw, T., Lidholm, S., Fitton, B., Beckman, J., Israel, F. P., Nieuwenhuijzen, H. & Vermue, J., 1981. *Astr. Astrophys.,* **102,** 257.
Dickel, H. R., 1974. *Astr. Astrophys.,* **31,** 11.
Elias, J. H., 1978. *Astrophys. J.,* **223,** 859.
Elias, J. H., Frogel, J. A. & Humphreys, R. M., 1985. *Astrophys. J. Suppl.,* **57,** 91.
Elias, J. H., Frogel, J. A., Hyland, A. R. & Jones, T. J., 1983. *Astr. J.,* **88,** 1027.
Elmegreen, B. G. & Lada, C. J., 1977. *Astrophys. J.,* **214,** 725.
Feinstein, A. J., 1982. *Astr. J.,* **87,** 1012.
Feinstein, A. J., Marraco, H. G. & Muzzio, J. C., 1973. *Astr. Astrophys. Suppl.,* **12,** 331.
Forte, J. C., 1978. *Astr. J.,* **83,** 1199.
Forte, J. C. & Orsatti, A. M. 1981. *Astr. J.,* **86,** 209.
Frogel, J. A., Persson, S. E., Aaronson, M. & Matthews, K., 1978. *Astrophys. J.,* **220,** 75.
Georgelin, Y. M. & Georgelin, Y. P., 1976. *Astr. Astrophys.,* **49,** 57.
Harvey, P. M., Hoffmann, W. F. & Campbell, M. F., 1979. *Astrophys. J.,* **227,** 114.
Herbst, W., 1976. *Astrophys. J.,* **208,** 923.
Hyland, A. R., 1974. In: *Highlights of Astronomy,* **3,** 307.
Hyland, A. R., Jones, T. J. & Mitchell, R. M., 1982. *Mon. Not. R. astr. Soc.,* **201,** 1095.
Isobe, S., 1971. *Ann. Tokyo astr. Obs.,* 2nd series, vol. XII, No. 3, 286.
Johnson, H. L., 1966. *Ann. Rev. Astr. Astrophys.,* **4,** 193.
Johnson, H. L., 1968. In: *Nebulae and Interstellar Matter,* p. 193, eds Middlehurst, B. M. & Aller, L. H., University of Chicago Press, Chicago.
Johnson, H. L., Mitchell, R. I., Iriarte, B. & Wisniewski, W. Z., 1966. *Communs Lunar planet. Lab.,* No. 63.
Jones, T. J. & Hyland, A. R., 1980. *Mon. Not. R. astr. Soc.,* **192,** 359.
Jones, T. J., Ashley, M., Hyland, A. R. & Ruelas-Mayorga, A., 1981. *Mon. Not. R. astr. Soc.,* **197,** 413.
Jones, T. J., Hyland, A. R., Robinson, G., Smith, R. & Thomas, J., 1980. *Astrophys. J.,* **242,** 132.
Landini, M., Natta, A., Oliva, E., Salinari, P. & Moorwood, A. F. M., 1984. *Astr. Astrophys.,* **134,** 284.
Lee, T. A., 1970. *Astrophys, J.,* **162,** 217.
Levato, H. & Malaroda, S., 1981. *Publs astr. Soc. Pacif.,* **93,** 714.
Lóden, L. O., Lóden, K., Nordström, B. & Sundman, A., 1976. *Astr. Astrophys. Suppl.,* **23,** 283.
Merrill, K. M. & Ridgeway, S. T., 1979. *Ann. Rev. Astr. Astrophys.,* **17,** 9.
Retallack, D. S., 1978. *Publs astr. Soc. Aust.,* **3,** 278.
Schultz, G. V. & Wiemer, W., 1975. *Astr. Astrophys.,* **43,** 133.
Stephenson, C. B. & Sanduleak, N., 1971. *Luminous Stars in the Southern Milky Way,* Publs Warner and Swasey Obs., Case Western Reserve University, Vol. 1, No. 1.
Thé, P. S. & Groot, M., 1983. *Astr. Astrophys.,* **125,** 75.
Thé, P. S., Bakker, R. & Tjin A Djie, H. R. E., 1980. *Astr. Astrophys.,* **89,** 209.

Thé, P. S., Arens, M., Groot, M. & Simon, K. P., 1982. In: *The Most Massive Stars,* p. 81, eds D'Ordorico, S., Baade, D. & Kjär, K., ESO Workshop, Garching.

Turner, D. G. & Moffat, A. F. J., 1980. *Mon. Not. R. astr. Soc.,* **192,** 283.

Walborn, N. R., 1973. *Astrophys. J.,* **179,** 517.

Walborn, N. R., 1982. *Astr. J.,* **87,** 1300.

Wamsteker, W., 1981. *Astr. Astrophys.,* **97,** 329.

Whittet, D. C. B. & van Breda, I. G., 1980. *Mon. Not. R. astr. Soc.,* **192,** 467.